



Improvement in Mechanical Properties of Mild Steel by Magnetically Induced Electrodeposition of Ni-Zn Alloy



Amna Hussain¹, Naseeb Ahmad^{1*}, Abdul Ghafar Wattoo¹ and Muhammad Imran¹

1Department of Physics, Khwaja Fareed University of Engineering and Information Technology, Pakistan

Submission: May 10, 2022; **Published:** June 22, 2022

***Corresponding author:** Naseeb Ahmad, Department of Physics, Khwaja Fareed University of Engineering and Information Technology, Rahim Yar Khan 64200, Pakistan

Abstract

Due to high cost and toxicity of cadmium coating, it can be replaced by Ni-Zn coating for various technological applications. The effect of Ni-Zn alloy coatings on mild steel under varying applied magnetic field from sulphate baths were studied using electrodeposition method. During deposition, steel substrate was taken as cathode and graphite rod was used as anode. Coating was performed using optimum operating parameters. Structure determination, surface morphology, thickness and mechanical properties were studied during this work. XRD results reveal that all the samples are single phase and have face centered cubic structure (fcc). The peak intensity increases with increasing magnetic field while lattice constant and crystallite size decrease up to the optimum value of magnetic field. The grain size becomes finer and more homogenous at specific applied magnetic field. Microhardness and other mechanical properties are improved by increasing applied magnetic field. Increase in magnetic field of Ni-Zn alloy coating improves the properties of steel which makes it more applicable in automotive, house building, electrical and aerospace industries. Coating through electrodeposition requires low cost, high deposition rate and easy to handle.

Keywords: Electrodeposition; Applied magnetic field; X-Ray diffraction; Surface morphology; Mechanical properties

Abbreviations: FCC: Face Centered Cubic Structure; FWHM: Full Width at Half-Maximum

Introduction

Cadmium has been utilized as a corrosion resistant coating in the aerospace, electrical, and fastener industries for many years due to its superior corrosion resistance and technical features [1]. However, Cd coatings in any form, are cancer-causing and pose a rising environmental and health risk; thus, Cd coating use is prohibited [2] in industrial applications. Zn coated steels have increased corrosion resistance in dangerous circumstances, but their service lifetimes are dramatically shortened due to the formation white rust [3,4]. When Zn is alloyed with Ni, the mechanical properties of the coating improve. Because of nickel's superior corrosion resistance, Ni-Zn alloy coatings are often employed to protect steel substrates [5]. It was also found that microhardness increased with the higher content of % Ni.

Recently, interest in Ni-Zn alloy coating has grown due to its superior mechanical and corrosion properties when compared to pure zinc coatings [6]. Developing and researching electrolytes of Ni-Zn alloy deposits is a high priority subject in electroplating. Many efforts have been made to better understand

the electrodeposition process and to improve its commercial uses under the influence of a superimposed magnetic field on deposit characteristics [7]. It was discovered that creating a magnetic field during the deposition process can modify the phase formation of the alloy coating [8,9]. Zinc is a diamagnetic metal, whereas nickel is a ferromagnetic metal. Magnetic force could effectively boost the deposition rate of nickel during the magnetic plating process, affecting the component of Ni-Zn alloy films [5].

For structural and morphological features for example, found that exerting an external magnetic field had a significant impact on the dendritic development of Zn and Ni. Smooth deposits have been described in some cases because of magnetic field [10]. However, as electromagnetic processing technology advances, researchers are increasingly focusing on obtaining alloy films in magnetic fields [11].

Mild steel has much application in construction, structural shapes for building and bridges, manufacture bolts, car bodies. Mild steel hardness is very tough in repairing and it rust easily.

This research aims to Ni-Zn alloy used for the replacement of high toxic cadmium in the application of the varied magnetic field. Mild steel has weak tensile strength, degradation with the passage of time and is not long-lasting. So, the coating of Ni-Zn alloy on mild steel enhances the mechanical property and to cost effect by the method of electrochemical deposition. The effect of Ni addition was studied and an improvement in hardness was observed. The hardening and stress properties of the inclusion of Ni alloy are improved.

In this present work we understand the effect of magnetic field on crystal orientation, hardening, stress properties and surface morphology. Zn-Ni alloy coatings have been studied using the same bath, focusing on magnetic field. In this work, Ni-Zn coatings have been deposited on mild steel, with a high content of Ni from sulphate bath by induced magnetic field B in the range of (0 to 4.5mT) in perpendicular direction. The variation of crystallite size, lattice parameter and surface smoothness were explained based

on magnetic field. An attempt was done to understand the effect of magnetic field on coatings properties like hardness, thickness, mechanical, morphological and crystallography structure.

Experimental procedure

Zn-Ni alloy prepared by electrodeposition method under the effect of varied magnetic field. Using laboratory-grade chemicals and double distilled water the solution bath was prepared. The coating solution for Ni-Zn alloys contained 30g/l H_3BO_3 , 50g/l zinc sulfate heptahydrate ($ZnSO_4 \cdot 7H_2O$) and 70g/l nickel sulfate heptahydrate ($NiSO_4 \cdot 7H_2O$), saccharin 1g/l. The bath elements and operating parameters of binary Ni-Zn alloy bath is listed in table 1. Graphite rod used as an anode and alloy coating was obtained on mild steel which is used as a cathode. Mild steel having area 2cmx1cm and it polished mechanically by emery paper of various grit sizes and cleaned by electrochemical solution.

Table 1: Concentration of used chemical with suitable operating parameters.

Chemicals	Concentration (g/l)	Operating parameters
$ZnSO_4 \cdot 7H_2O$	50	Deposition time: 20 min Current density: 2.0 Adm⁻² Magnetic field intensity: 0.0 to 4.5 mT pH: 3.0 Temperature: 293K
$NiSO_4 \cdot 7H_2O$	70	
H_3Bo_3	30	
Saccharin	1	

The pH was adjusted by the addition of Boric acid solution to perform Zn-Ni deposits at pH=3 and tested by pH paper meter and all deposition was conceded at room temperature for 20min. The deposit current density was kept constant (2.0 A/cm²) for study the effect of external applied magnetic field. The magnetic field of known intensity was applied. The magnetic field parallel to the electrodes and a constant distance was maintained between cathode and anode. The electrolytic cell was kept in the gap of electromagnets perpendicular was introduced during the electroplating process to obtain Ni-Zn thin alloy films on a steel substrate. The magnetic field applied was found to be uniform and homogeneous in the region of electrolysis.

The phase structure, crystallite size and crystallographic orientation of Zn-Ni alloy was investigated using the method of X-ray diffraction using Cu-K α ($k = 1.5406 \text{ \AA}$). The microstructural characterization and surface morphology of the coating was

studied using scanning electron microscope (Hitachi-S3400). Mechanical properties are testing by (Shimadzu-AGX-057B machine) and Vickers hardness tester by AKASHI (HM-102) analyzed the microhardness and average roughness of the coating.

Results and Discussion

Thickness of coating is calculated by the mass difference before and after the deposition on substrate. Data of the calculated thickness, deposited mass for Ni-Zn coatings is given in the table 2. The data in the table values gives information about the changes which produced in substrate after deposition by applying magnetic field. It is being noted in table 2 that the deposited mass increases with the applied magnetic field [12] the film thickness also increases as well, eventually reaching a maximal position value at 20mint deposition time. The greatest film thickness measured in this study was determined to be 73 μ m (figure 1).

Table 2: Influence of magnetic field on thickness and deposited mass for Ni-Zn alloy coatings.

Sample no	Magnetic field (mT)	Deposited mass (g)	Thickness (μ m)
1	0	0.03	36.8
2	1.5	0.04	49.1
3	3	0.05	61.4
4	4.5	0.06	73.7

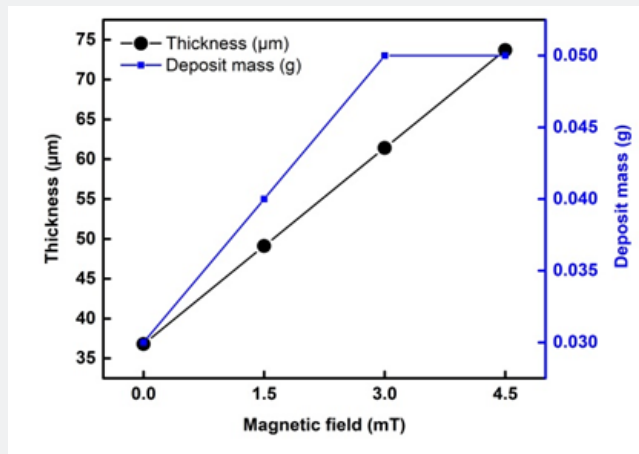


Figure 1: Variation in thickness and deposited mass with change in magnetic field.

A very slight difference is observed in the thickness of the coated steel substrate. The increase in thickness is due to more deposited mass by applying magnetic field [13]. By increasing the deposit mass, the thickness of the substrate is increased then the smoothness of the surface is decrease. So, when the thickness increases to 70% then the deposit Ni-Zn alloy show some cracks on the surface. As in SEM result at higher magnetic field ($B=4.5\text{mT}$) surface shows some cracks similar when the thickness beyond to 70% at higher magnetic field surface shows cracks. In XRD the peaks of the intensity also decrease at higher magnetic field compared to other lower magnetic field due to increasing thickness. The Ni-Zn alloy is noted for being brittle and hard. The rise in thickness with the magnetic field is the cause of the crack

[14].

X-ray diffraction is studied to investigate the crystal structure of deposited Ni-Zn alloy. The XRD patterns obtained from the sulfate baths in which Ni-Zn alloy coatings are of a mild steel substrate. Graphs are created to show the relationship between intensity and 2θ range. The structural parameters such as crystallite size (D), lattice constant (a) and d-spacing (d) can also be discussed. With the help of X-ray diffraction patterns three peaks could be seen (111), (200) and (220) at 42° , 49° and 72° in the range of 2θ angles from 30° to 80° . Which demonstrate that Ni-Zn coating has face centered cubic crystal (fcc) which is determined using standard method.

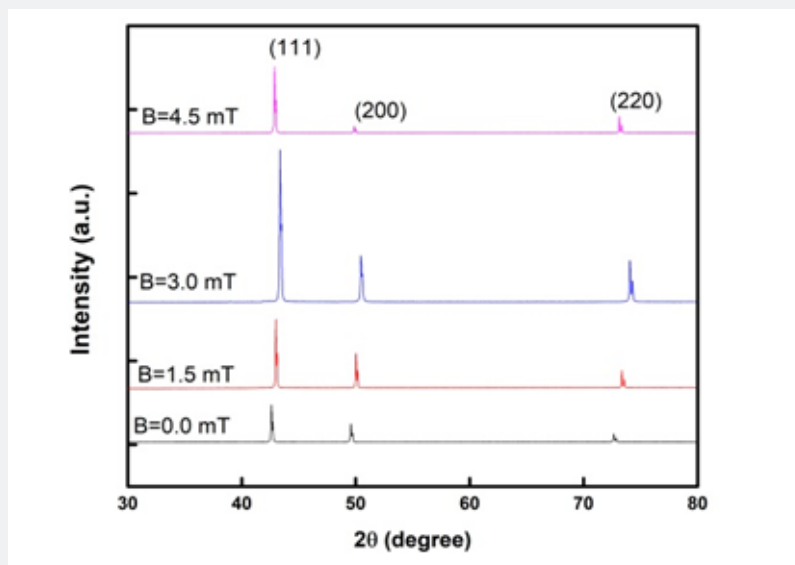


Figure 2: XRD pattern with miller indices of Ni-Zn alloy coating (a) at 0.0mT (b) 1.5mT, (c) at 3.0mT, (d) at 4.5mT.

Figure 2 shows a comparative relation of X-ray diffracted intensity peaks of Ni-Zn alloy. The peak intensity alters significantly with changes in applied magnetic field strength. As shown in figure 2 that all the peaks shifted from lower to higher angles of 2θ range with different values of intensity which is due to residual stress that can shifted some peaks in different directions. Diffracted peak intensity increases with the increasing of applied magnetic field [15]. Magnetic field at 0 and 4.5mT, peaks of the plane (111) seem to be less broadening due to increasing crystallite size but at 1.5 and 3.0mT magnetic field the peaks are sharp and broaden due to decreasing crystallite size.

As we move towards higher angle the intensity of the peaks going to decrease but sharply increase by increasing of magnetic field. Furthermore, Chiba et al. concluded from XRD study that magnetic field repair crystal growth, this effect is more dominant at low magnetic field and this effect is more dominant at optimum magnetic field. Peaks intensity along the planes (111), (200) and (220) increasing continuously up to 3mT magnetic field but this intensity decreases at 4.5mT, hence 3mT is the optimum value of magnetic field [16]. No new peaks have developed because of

the applied magnetic field, except for the increase in diffracted intensity as the magnetic field strength increases, as illustrated in figure 2.

The phase structure, crystallite size and crystallographic orientation of Zn-Ni alloy was investigated using the method of X-ray diffraction using Cu-Kα (k = 1.5406 Å) as copper source. All the coated samples were scanned in 5° to 80° (2θ) diffraction angle range, with a step size of 0.05° and scanning rate of 0.01/°s. Crystallite size (D) which is a single smallest crystal in size was calculated using the Scherrer equation:

$$D = \frac{(0.9\lambda)}{(\beta \cos^{\theta})} \dots\dots\dots (1)$$

Where k=0.9 is the Scherrer constant, λ is the wavelength of copper source (λ= 1.5406) in Angstrom (Å), β is determined by XRD data the full width at half-maximum (FWHM) of the peak, and θ is the diffraction angle are also known as Bragg's angle measured in radians, respectively. Data about crystallite size, lattice parameter and d-spacing for all samples under varying magnetic field is given table 3 (figure 3).

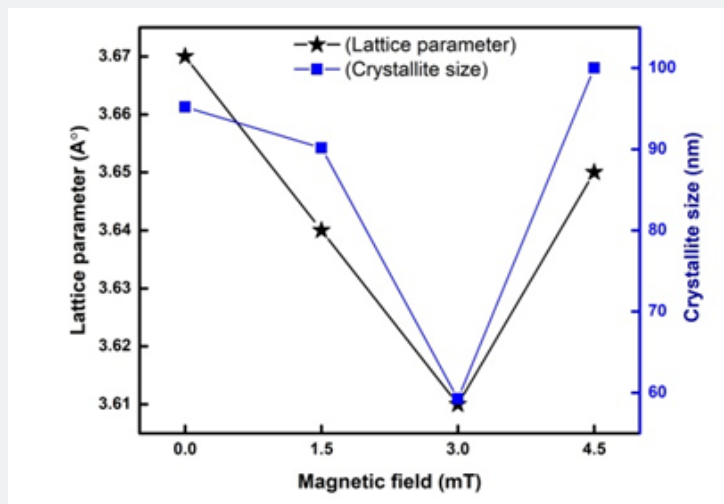


Figure 3: Variation of the Lattice constant and crystallite size of Ni-Zn alloy at different magnetic field.

Table 3: Structural parameters of Ni-Zn alloy coating at different magnetic field.

Sample no	Magnetic field (mT)	d-Spacing (Å)	Crystallite size (nm)	Lattice Constant. a(Å)
1	0	1.75	95.21	3.67
2	1.5	1.73	90.15	3.64
3	3	1.72	59.26	3.61
4	4.5	1.74	100.01	3.65

The crystallite size of the coatings is calculated using the Scherer formula used in chapter 3 and found to be decreasing from 95nm to 59nm [17] with increasing in magnetic field to the optimum value. With increasing magnetic field, it observes decreasing in lattice parameter from 3.67 to 3.61 Å and same

behavior in d-Spacing from 1.75 to 1.72 Å. But at high magnetic field the crystallite size increased to 100.01 Å [15], d- spacing and lattice parameter increased 1.74 Å and 3.65 Å respectively at high magnetic field 4.5mT [16].

Increase in nucleation rate cause the crystallite size to shrink [18]. This decreasing of crystallite size makes the surface smooth, compact and durable. Smaller crystallite size is responsible to higher mechanical properties. The change in magnetic field had a considerable impact on their crystallite size, which changed the surface morphology as a result [19].

The microstructural characterization and surface morphology

of the coating was studied using scanning electron microscope (SEM-Hitachi S3400). The grain size of the sample was also determined directly by help of SEM to verify the accuracy of the average grain size measurements. Without magnetic field as seen in figure 4(a) particle have high grain size and non-uniform surface morphology and high grain size but when a magnetic field is applied, the grain size becomes finer and more homogenous [16].

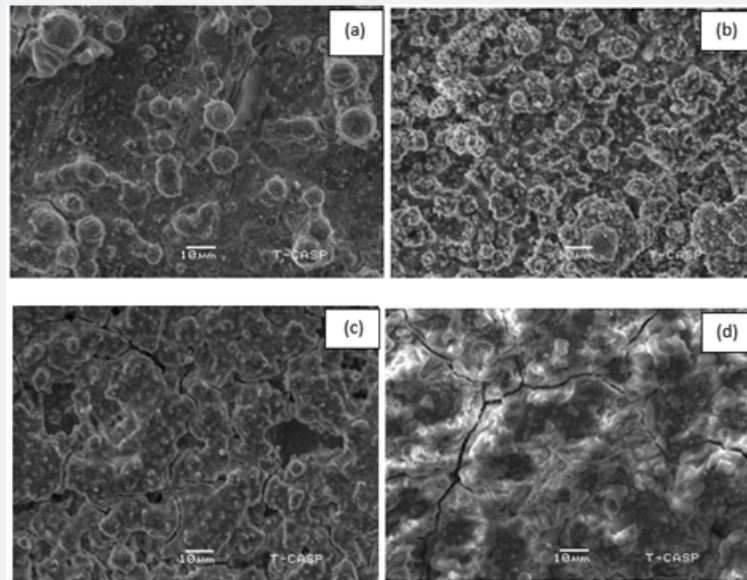


Figure 4: Ni-Zn SEM micrographs deposited (a) at 0.0mT (b) 1.5mT, (c) at 3.0mT, (d) at 4.5mT magnetic field.

The average particle grain size was estimated from SEM micrograph and found to be 7.51, 7.45, 7.30 and 8.26 (μm) at magnetic field $x = 0.0$ and 1.5, 3.0 and 4.5mT respectively. At figure 4(a) Without magnetic field the surface morphology is non-uniform. The average grain size is 7.51 (μm) at 0mT magnetic field. In figure 4(b) the average grain size is 7.45 (μm) at 1.5mT magnetic field. At low magnetic field (1.5mT), the Ni-Zn coating exhibits a cauliflower-like spherical shape as illustrated in figure 4(b). This micron-sized cauliflower-like structure was dense, compact, and crack-free.

In figure 4(c) magnetic field at 3mT found to be coated with homogeneous void growths [8]. The average grain size is 7.30 (μm) for this Ni-Zn alloy sample. The grain size continuous reduces up to $B=3.0\text{mT}$ magnetic field. Although little voids are produced but overall coating is going to smooth [20] figure 4(d) the average grain size is 8.26 μm at high magnetic field 4.5mT. With increasing magnetic field, the grain size increased which lead to the formation of micro-cracks, as seen figure 4(d) [21]. The reason of the cracks was not clearly visible. Jessen proposed a sensible reason, stating that the cracks were produced because of stresses developed during Zn dissolution in the deposition [22].

Table 4 indicates that without magnetic field surface is non-uniform and high grain size. But the applied magnetic field, surface become smooth, compact, hard and cauliflower spherical shape. By the presence of magnetic field resulting decrease in grain size which responsible to fine grain morphology. It could be owing to the grain refinement generated by the variation of magnetic field. Further, increase in magnetic field 4.5mT, grain size is increased due to cracks and void as shown in figure 4(d).

The particle grain size determined by SEM and they all are agreeing well with the crystallite size recorded by XRD [23]. Mechanical properties of material tell how long a material bear stress, how hard a material, and how elastic a material. Detail of mechanical properties like microhardness, yield stress, ultimate tensile strength, elastic modulus, and elongation are analyzed in the coming section.

Hardness is a material's ability to resist against deformation. Vicker's hardness is calculated by the help of diamond pyramid shaped indenter. The tensile strength of a metal determines its capacity to bear tensile loads without breaking. When a material is stretched or pushed, it can withstand the most stress before breaking (table 5). Data in the table shows that by increasing

applied magnetic field, the values of microhardness and ultimate tensile strength increases and it continuously show direct relation with magnetic field [24]. Variation in graph is reasonable to the

variation of magnetic field which varies significantly during deposition (figure 5).

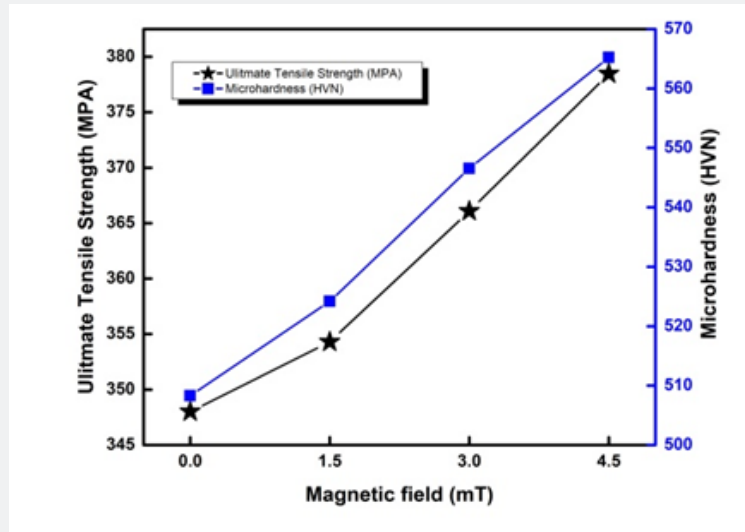


Figure 5: Variation in microhardness and ultimate tensile strength with change in magnetic field of Ni-Zn alloy coating.

Table 4: Variation of grain size under the effect of applied magnetic field.

Sample no	Magnetic field (mT)	Grain size (um)
1	0	7.51
2	1.5	7.45
3	3	7.3
4	4.5	8.26

Table 5: Influence of magnetic field on microhardness and ultimate tensile strength for Ni-Zn alloy coating.

Sample No.	Magnetic field (mT)	Microhardness before deposition (HVN)	Microhardness after deposition (HVN)	UTS before deposition (MPa)	UTS after deposition (MPa)
1	0	254.798	508.292	336.09	348.009
2	1.5	254.798	524.194	336.09	354.302
3	3	254.798	546.527	336.09	366.089
4	4.5	254.798	565.221	336.09	378.466

Any substrate with a high hardness has shown to be extremely resistant to corrosion and scratches [25]. The average increment of microhardness and ultimate tensile strength is 109 and 19 % respectively. The tensile strength of a material is proportional to its hardness. Any specimen with a high hardness seems to have a high tensile strength, which means that great stress is required to fracture it. As a result, increasing the hardness of the substrate improves the tensile strength. Resistance to permanent deformation is called yield stress. The ratio of the stress applied to the resulting stress is called the elasticity module. It is also

defined as elastic deformation resistance (table 6).

Increase in yield stress also responsible to better corrosion protection. Tensile strength is directly proportional to yield stress [26] (figure 6). Elastic modulus and the yield stress improved by decreasing the crystallite size [27]. By increasing the hardness, the elastic modulus also increased because both are proportional [28] its means that if stress is applied to the material, it does not break or deform. High tensile stress means it resist the external applied force, without breaking. Elongation is the percentages changes in the length to the original length (table 7).

Table 6: Influence of magnetic field on yield stress and elastic modulus for Ni-Zn alloy coating.

Sample No.	Magnetic field (mT)	Yield Stress before deposition (MPa)	Yield Stress after deposition (MPa)	Elastic Modulus before deposition (Gpa)	Elastic Modulus after deposition (Gpa)
1	0	240.88	295.656	200.552	231.523
2	1.5	240.88	299.102	200.552	245.34
3	3	240.88	305.767	200.552	249.213
4	4.5	240.88	308.994	200.552	252.985

Table 7: Influence of magnetic field on elongation for Ni-Zn alloy coating.

Sample No.	Magnetic field (mT)	Elongation before deposition (%)	Elongation after deposition (%)
1	0	18.309	35.908
2	1.5	18.309	37.123
3	3	18.309	38.325
4	4.5	18.309	39.98

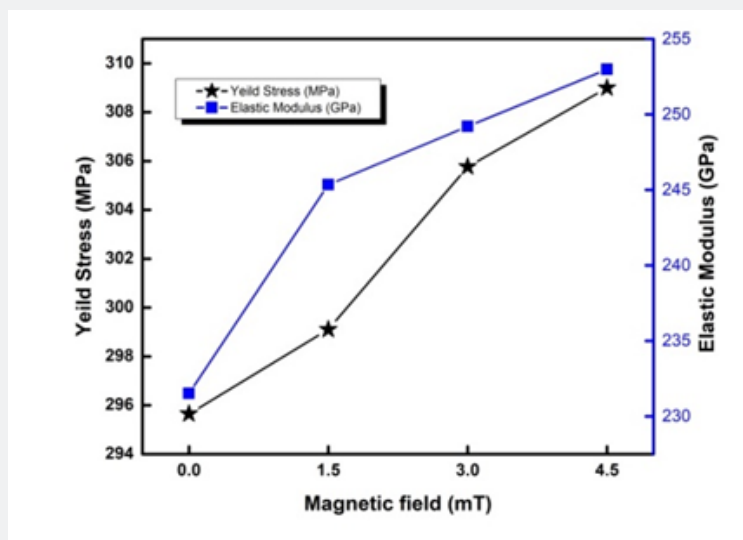


Figure 6: Variation in yield stress and elastic modulus with change in magnetic field of Ni-Zn alloy coating.

The data in the table gives the information of the improvement in elongation of the substrate after the deposition. This value shows that by increasing magnetic field the elongation is increased. As the SEM micrograph showed the grain size decrease as the magnetic field increase due to which elongation also increase. Which means it increases ductility of the alloy [29] (figure 7). The graphical representation shows that magnetic field make good impact on steel substrate by the high value of elongation [2]. The bath prepared under magnetic field shows maximum elongation compared to another bath. Ductility increased under magnetic field with the maximum elongation at same temperature [30]. It can also be noticed that by decreasing grain size in SEM result the

elongation of the substrate increases under the effect of magnetic field (figure 8).

Without magnetic field the microhardness of the sample is very low but when applying magnetic field, the microhardness of the Ni-Zn coated mild steel suddenly increases. Also, the value of ultimate tensile strength, yield stress and elastic modulus, elongation increases with the increasing magnetic field. When magnetic field is applied, these values increases and it continuously show direct relation with magnetic field. Variation in graph is reasonable to the variation of magnetic field in the bath which varies significantly during deposition.

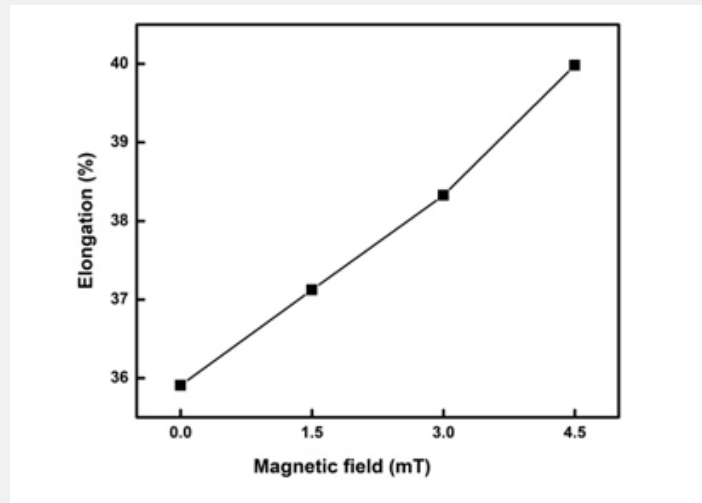


Figure 7: Variation in Elongation with change in magnetic field of Ni-Zn alloy coatings.

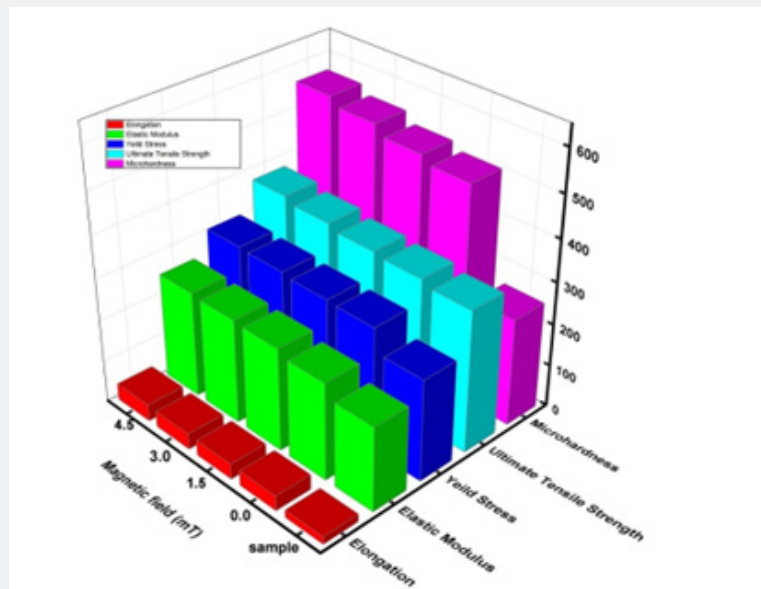


Figure 8: Combined graph of Mechanical properties of Ni-Zn alloy coatings deposited at different magnetic field.

Conclusion

Ni-Zn alloy coatings deposited by electrodeposition on mild steel from a sulphate bath are studied. The effect of variation of magnetic field on crystal structure, surface morphology as well as mechanical properties like hardness and thickness is considered. When applied magnetic field is increased, the deposit mass of the coated substrate is continuously increased and hence, the thickness of coating is increased continuously. The peak intensity increases with the increasing of magnetic field up-to the optimum value and XRD diffracted line showed a single face cubic crystal structure (fcc). The plane intensity of (111) is dominant from all

other planes peaks due to small, diffracted angle.

In XRD, crystallite size, lattice constant and d-spacing decrease with increasing magnetic field and further increasing magnetic field they all are increases. SEM results show that more compact morphology of the coating obtained at magnetic field of 3.0mT. The hardness of the coating increased with varying magnetic field and it improved the strength and ductility of the steel. The hardness and all other mechanical properties yield stress, elongation, ultimate tensile strength, and modulus of elasticity of Ni-Zn alloy coatings increased as the applied magnetic field is increased. All the coated property showed best behavior at optimum magnetic

field ($B=3\text{mT}$) at higher magnetic field they show inverse behavior as XRD and SEM results show but mechanical properties increasing continuously as the applied magnetic field increases.

References

1. Lohitha B, Thanikaikarasan S, Marjorie SR (2020) Structural and optical properties of electroplated cadmium sulphide thin films. *Materials Today: Proceedings* 33: 3405-3408.
2. Tian Z, Zhang L, Fu S, Yuan R, Dong Z, et al. (2016) The effect of magnetic field intensity and treatment time on graphene/epoxy composites' fracture toughness. *IOP Conf Ser Mater Sci Eng* pp.137.
3. Rajagopalan SK (2012) Characterization of electrodeposited Zn-Ni alloy coatings as a replacement for electrodeposited Zn and Cd coatings. Montreal: McGill University.
4. Kalendova A (2003) Comparison of the anticorrosion efficiencies of pigments based on condensed phosphates and polyphosphosilicates. *Anti-Corrosion Methods and Materials* 50(2): 82-90.
5. Krause A, Hamann C, Uhlemann M, Gebert A, Schultz L (2005) Influence of a magnetic field on the morphology of electrodeposited cobalt. *Journal of magnetism and magnetic materials* 290: 261-264.
6. Shivakumara S, Manohar U, Naik YA, Venkatesha T (2007) Influence of additives on electrodeposition of bright Zn-Ni alloy on mild steel from acid sulphate bath. *Bulletin of Materials Science* 30(5): 455-462.
7. Krstajić N, Jović VD, Gajić-Krstajić L, Jović BM, Antozzi A, et al. (2008) Electrodeposition of Ni-Mo alloy coatings and their characterization as cathodes for hydrogen evolution in sodium hydroxide solution. *International Journal of Hydrogen Energy* 33(14): 3676-3687.
8. Ispas A, Matsushima H, Plieth W, Bund A (2007) Influence of a magnetic field on the electrodeposition of nickel-iron alloys. *Electrochimica acta* 52(8): 2785-2795.
9. Uhlemann M, Krause A, Chopart J, Gebert A (2005) Electrochemical deposition of Co under the influence of high magnetic fields. *Journal of the Electrochemical Society* 152(12): C817.
10. Koza JA, Uhlemann M, Gebert A, Schultz L (2008) The effect of magnetic fields on the electrodeposition of CoFe alloys. *Electrochimica acta* 53(16): 5344-5353.
11. Yu Y, Wei G, Hu X, Ge H, et al. (2010) The effect of magnetic fields on the electroless deposition of Co-W-P film. *Surface and Coatings Technology* 204(16-17): 2669-2676.
12. Sanaty-Zadeh A, Raeissi K, Saidi A (2011) Magnetic properties of nanocrystalline Fe-Ni alloys synthesized by direct and pulse electrodeposition. *International Journal of Modern Physics B* 25(15): 2031-2038.
13. Maria Białostocka A, Klekotka U, Kalska-Szostko B (2019) Modulation of iron-nickel layers composition by an external magnetic field. *Chemical Engineering Communications* 206(6): 804-814.
14. Ul-Hamid A, Quddus A, Al-Yousef F, Mohammed A, Saricimen H, et al. (2010) Microstructure and surface mechanical properties of electrodeposited Ni coating on Al 2014 alloy. *Surface and Coatings Technology* 205(7): 2023-2030.
15. Shetty S, Hegde AC (2017) Magnetically induced electrodeposition of Ni-Mo alloy for hydrogen evolution reaction. *Electrocatalysis* 8(3): 179-188.
16. Chouchane S, Levesque A, Douglade J, Rehamnia R, Chopart JP (2007) Microstructural analysis of low Ni content Zn alloy electrodeposited under applied magnetic field. *Surface and Coatings Technology* 201(14): 6212-6216.
17. Rashmi S, Elias L, Hegde AC (2017) Multilayered Zn-Ni alloy coatings for better corrosion protection of mild steel. *Engineering science and technology, an international journal* 20(3) 1227-1232.
18. Abou Krisha MM (2012) Effect of pH and current density on the electrodeposition of Zn-Ni-Fe alloys from a sulfate bath. *Journal of Coatings Technology and Research* 9(6): 775-783.
19. Rashmi D, Pavithra G, Praveen B, Devapal D, Nayana K, et al. (2020) Electrodeposition of Zn-Ni monolithic coatings, characterization, and corrosion analysis. *Journal of Failure Analysis and Prevention* 20: 513-522.
20. Rahman M, Sen S, Moniruzzaman M, Shorowordi K (2009) Morphology and properties of electrodeposited Zn-Ni alloy coatings on mild steel. *Journal of Mechanical Engineering* 40(1): 9-14.
21. Beheshti M, Ismail MC, Kakooei S, Shahrestani S (2020) Influence of temperature and potential range on Zn-Ni deposition properties formed by cyclic voltammetry electrodeposition in chloride bath solution. *Corrosion Reviews* 38(2): 127-136.
22. Alfantazi A, Erb U (1996) Corrosion properties of pulse-plated zinc-nickel alloy coatings. *Corrosion* 52(11): 880-888.
23. Kumar R, Kumar H, Singh RR, Barman P (2016) Variation in magnetic and structural properties of Co-doped Ni-Zn ferrite nanoparticles: a different aspect. *Journal of Sol-Gel Science and Technology* 78(3): 566-575.
24. Rao VR, Bangera K V, Hegde AC (2013) Magnetically induced electrodeposition of Zn-Ni alloy coatings and their corrosion behaviors. *Journal of magnetism and magnetic materials* 345: 48-54.
25. Sriraman K, Strauss H, Brahimi S, Chromik R, Szpunar J, et al. (2012) Tribological behavior of electrodeposited Zn, Zn-Ni, Cd and Cd-Ti coatings on low carbon steel substrates. *Tribology International* 56: 107-120.
26. Fashu S, Khan R (2019) Recent work on electrochemical deposition of Zn-Ni (-X) alloys for corrosion protection of steel. *Anti-Corrosion Methods and Materials* 66(1): 45-60.
27. Rashmi D, Pavithra G, Praveen B, Devapal D, Nayana K, Hebbar SP (2020) Characterization and Corrosion Analysis of Electrodeposited Nanostructured Zn-Fe Alloy Coatings. *Journal of Bio-and Tribo-Corrosion* 6: 84.
28. Wasekar NP, Bathini L, Ramakrishna L, Rao DS, Padmanabham G (2020) Pulsed electrodeposition, mechanical properties and wear mechanism in Ni-W/SiC nanocomposite coatings used for automotive applications. *Applied surface science* 527: 146896.
29. Jiao ZB, Luan JH, Liu CT (2016) Strategies for improving ductility of ordered intermetallics. *Progress in Natural Science: Materials International* 26(1): 1-12.
30. Huang C, Zou M, Qi L, Ojo OA, Wang Z (2021) Effect of Isothermal and Pre-transformation Temperatures on Microstructure and Properties of Ultrafine Bainitic Steels. *Journal of Materials Research and Technology* 12: 1080-1090.



This work is licensed under Creative Commons Attribution 4.0 License
DOI: [10.19080/IMST.2022.03.555610](https://doi.org/10.19080/IMST.2022.03.555610)

**Your next submission with Juniper Publishers
will reach you the below assets**

- Quality Editorial service
- Swift Peer Review
- Reprints availability
- E-prints Service
- Manuscript Podcast for convenient understanding
- Global attainment for your research
- Manuscript accessibility in different formats

(Pdf, E-pub, Full Text, Audio)

- Unceasing customer service

Track the below URL for one-step submission

<https://juniperpublishers.com/online-submission.php>